*International Journal of Information Technology and Knowledge Management*
*July-December 2008, Volume 1, No. 2, pp. 337-350*

# QUALIFYING FIBRE OPTIC TEMPERATURE SENSOR USING SPECKLE METROLOGY

**Bhasker Gupta, H. N. Bhargaw & H. K. Sardana**

## Abstract

A distributed temperature sensing approach based on laser speckles in multimode fibres is characterised. The speckle patterns are intensity distributions of different modes formed by the interference of the modes from a coherent source. The system design involves the use of an optical signal transmitter unit, the sensing fibre and a receiver unit. The receiver unit consists of a camera with a "diffuser glass in tube arrangement". A CCD camera housed in the receiver unit receives the speckle image, which is grabbed by image acquisition hardware and computer for analysis. The slowly varying perturbation such as temperature is appropriate for qualifying the sensor. The sensor uses Cu-coated fibre for enhancing the performance. Two image processing algorithms have been used for characterisation of two sensing configurations. Results have been generated in terms of sensitivity, working range, system response time.

***Keywords:*** Correlation, fibre-optic sensors, MSV, response time, sensitivity, sensing configurations, Speckle patterns, working range.

## I. Introduction

Fibre optic sensors are of interest now for more than two decades[1-3]. Multimode fibres are more frequently used than single mode fibres which are particularly suited for communication. When a fibre is subjected to temperature perturbations, it experiences geometrical (size, shape) and optical (refractive index, mode conversion) changes to a larger or lesser extent depending upon the nature and the magnitude of the perturbation [4]. Fibres are characterized [5] by their loss as a function of wavelength, their numerical aperture, the core diameter, and their mechanical properties including the external diameter, the coatings and the manner in which the fibre is finally cabled. While this approach obviously saturates the working range of the sensor till the physical limits. The work presented here uses fibre speckles for transforming the energy due to perturbations. In this approach, the most sensitive inter-modal interference is exploited wherein though the working range is very small, but fortunately the speckle patterns change in a cyclic manner thus permitting reusability of the sensor [1] for wider range by repeated shifts of the reference pattern. This work further emphasizes the design of sensors by choosing appropriate layout that encompasses a field rather than a point. In addition, extra metal coated on the exterior surface of the fibre enhances energy gathering

while using them as thermal sensors. Such distributed sensing of temperature may arise from an operating engine, machinery or an industrial process.

## 2. FIBRE SPECKLE METROLOGY

Granular structure formed in space when coherent light is scattered or transmitted through an optically rough surface is called a speckle pattern [6]. The for-mation of a speckle pattern is not unique to visible radiation; it also has been observed in other parts of the electromagnetic spectrum. The inter-modal dispersion property of multimode fibre creates this phenomenon. In other words the speckle patterns or model noise [7] are formed by the interference of the modes from a coherent source when a coherent time of the source is greater than the inter-modal dispersion time within the fibre.

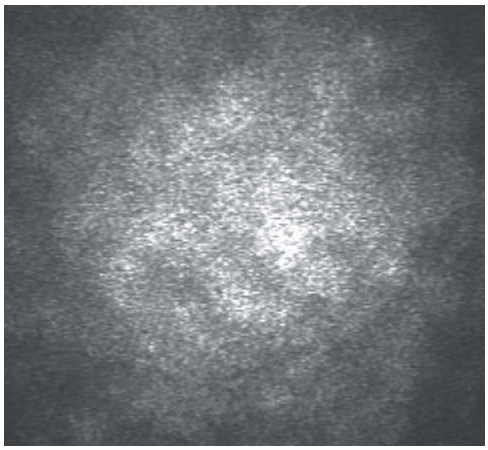

**Figure 1: Speckle Pattern**

The conditions which generate the speckles are therefore specified as [7]:

(1) A coherent source with a narrow spectral width and long coherence length (propagation velocity multiplied by the coherence time)

(2) Distribution along the fibre which gives differential mode delay and spatial filtering.

(3) Phase correlation between the modes.

The actual structure of the speckle pattern depends on the coherence proper-ties of the incident field and also on the surface characteristics of the rough (target) object. Speckle pattern of a multimode fibre output is an interference pattern produced by the superposition of the model phase distribution

When the output from a multimode fibre is projected on a screen (e.g. glass plate), a uniform circular pattern is observed (Fig. 1). Although speckle patterns also exist when the light is incoherent but there is a smooth distribution of intensity within the pattern. When coherent light is used, however, the pattern becomes very granular and consists of a very large number of speckles of varying intensities. The distribution of these speckles changes slowly over time, but the intensity of the total circular pattern remains basically constant. When the optical fibre carrying the coherent light is perturbed, the distribution of the speckle intensities change with the perturbation, with some speckles becoming brighter, some dimmer and some not changing at all. The total intensity of the pattern remains unchanged; however an analysis of the changes in the speckle pattern can be used to obtain information about the perturbation of the fibre [2]. When light of wavelength $\lambda$ is launched into the fibre of core diameter, $D = 2a$ and core refractive index $n_1$ and cladding refractive index $n_2$ the total number of guided modes, $M$ can be estimated from the normalized frequency [8]:

$$V = 2\pi a \frac{(n_1^2 - n_2^2)^{1/2}}{\lambda} \tag{1}$$

For the case in which $a/\lambda >> 1$, $M$ may be approximated to

$$M \cong V^2/2 \tag{2}$$

These modes travel through different optical paths and at the other end of fibre they interfere with each other give rise to a speckle pattern.

Of interest to speckle metrology is the average speckle size. The statistical average size of the speckle diameter of a light field formed by an optical fibre in the plane placed at a distance $R$ from its output can be calculated as

$$S_D = 2.44.R.\left(\lambda/D\right) \tag{3}$$

Thus the entire number of light and dark speckles in the pattern can be calculated as

$$\text{Total no of light and dark patterns} = \left(NA^2.D^2\right)/\lambda^2 \tag{4}$$

Where $NA$ is the numerical aperture of the fibre and $S_D$ is average size of speckle $R$ is the distance between the fibre ends and the detector plane and $D$ is diameter of the fibre [7].

## 3. PERTURBATION SENSING SETUP

The setup used for temperature sensing is a variant of a system that can be used to sense various other external perturbations like pressure, vibration, displacement, stress/

strain etc within a number of zones [9]. This existing system consists of transmitter section and receiver section as shown in Fig. 2 Laser light (635nm) is coupled in to the multimode fibre through specially designed connectors.

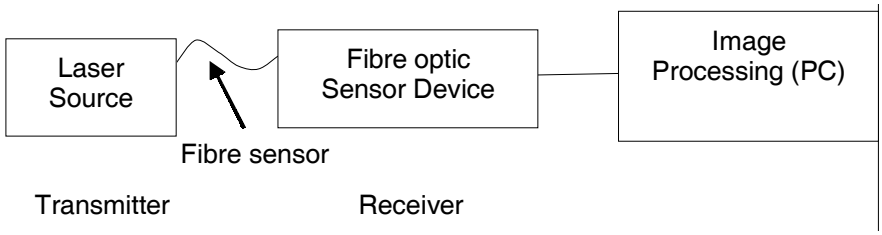


**Figure 2: Schematic Diagram of the System**

The main component of sensing system is multimode fibre (MMF). Core and cladding diameter of a commercial Cu-coated fibre is 50 and 125 μm respectively and *NA* is 0.22 ± 0.02. Its operating temperature range is –270°C to +700°C. Both ends of this fibre sensor are terminated with standard connecters. The laser diode emits coherent light into the sensor fibre of sufficient length. While on receiver side it consisting of Sensor Device (SD), CCD camera and image processing unit. Sensor device contain diffuser glass plate and C-mount imaging lens as shown in Fig. 3.

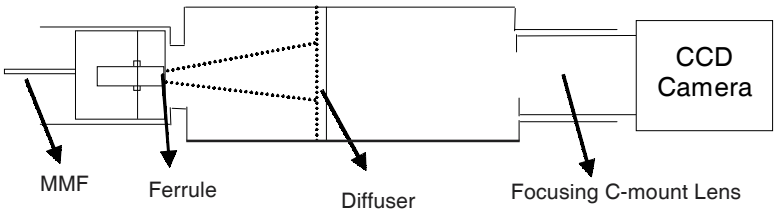


**Figure 3**: **Schematic Diagram of Sensor Device**

Fibre holder is mounted on the front side of the device and this is sliding in to the outer housing of the device. This device has been designed and developed for 2-D array multi zone perturbation sensing system and can be used for sensing perturbations due to varying temperature based on speckle image pattern.

## 4. STATISTICAL ANALYSIS ALGORITHMS

The output speckle patterns are affected by external perturbations and to measure these perturbations an approximate relationship between the perturbing factor and the speckle intensity distribution has to be determined. Following statistical parameters are used for speckle image analysis.

### 4.1. The MSV Measurement

It is implemented or detected by absolute pixel wise difference [1, 2] between the initial and current images of speckle patterns. The overall intensity of difference image is then integrated to obtain normalized assessment of perturbations.

Let the initial status of the fibre is $S_o$ and new changed fibre status is $S$. thus the intensity variation between status $S_o$ and status $S$ at point $Q$ can be determined by

$$\Delta I\,(x, y) = I_o\,(x, y) - I\,(x, y) \tag{5}$$

Where $(x, y)$ are the spatial coordinates at the observation plane, $I_o$ and $I$ are the intensity at the observation point caused by the initial and the subsequent states of the fibre. The mean absolute speckle intensity variation can be approximated by integrating over the speckle field as

$$\text{MSV} = \iint \Delta I \mid dxdy \tag{6}$$

Where $\Delta I$ is the pixel wise intensity difference between the current and subsequent speckle image(s). This method of implementation is highly sensitive and accurate.

### 4.2. Correlation Measurement

When the sensing fibre is subjected to perturbation, the optical path length of propagating modes undergoes changes. These changes can be detected [3,8] by comparing the resulting pattern with a reference pattern. The correlation parameter [10, 11] is obtained between the reference speckle image and varying perturbation speckle images. This correlation values represent the signal values of the perturbations. The $I_0\,(x, y)$ is the intensity at a point of coordinate $(x, y)$ of the initial (or reference) and $I\,(x, y)$ is the intensity at the corresponding point under perturbation. The spatial correlation between the two images is:

$$\rho(I_0, I) = \tfrac{1}{K} \sum_{x,y}^{N} I_0(x,y) * I(x,y) \tag{7}$$

$K$ is the normalized constant for the image size ($NxN$).

$$K = \sum_{x,y}^{N} I_0(x,y).I(x,y) \tag{8}$$

The correlation parameter has unity value if the intensity pattern is correlated with the reference and decreases gradually as the applied perturbation increases.

## 5. TEMPERATURE SENSING CONFIGURATIONS

For experimenting with temperature perturbations two configurations were designed to interface temperature perturbation directly to sensing fibre. For this purpose, sensing fibre should be embedded on some material that has high thermal conductivity. Cu plate was chosen as the base material and for fixing fibre on plate, a single U-shape groove was made covering the desired area and also maintaining bending radius of fibre. For inducing temperature perturbation Cu plate was heated by using a reference thermometer and heating equipment (soldering station with temperature control). In another configuration, the setup was made more sensitive to temperature perturbation by laying extra length of the fibre. Therefore, three fibre turns were mounted in the form of a spiral rather than one. Two such configurations were made by placing fibre in the grooves and soldered as shown in Fig. 4.

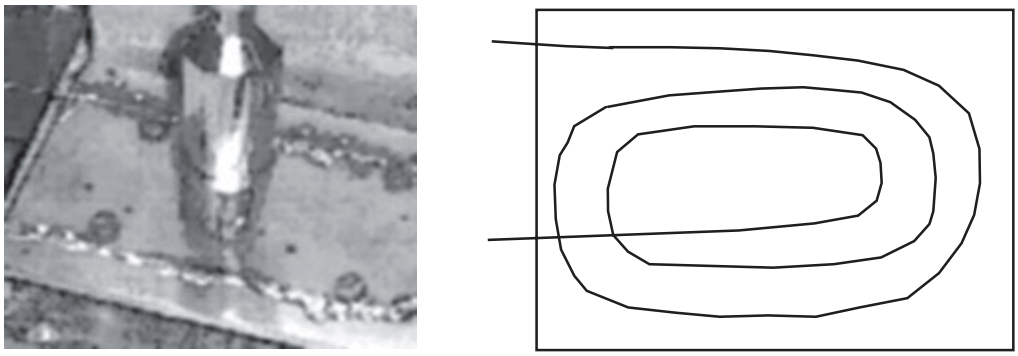

**(a)** **(b)**

**Figure 4: Sensing Configurations (a) Single-turn with Thermometer (12cm) (b) Three-turn (26cm)**

## 6. EXPERIMENTS AND RESULTS

Experimentation was done in both rise and fall of temperature with both developed temperature sensing configurations, but in this paper results with increasing temperature are shown. Experimentation is started by heating sensing module with standard heating equipment with reference thermometer. Two experiments were conducted for single-turn configuration by heating it in the range (35–66.4°C) and three-turn in the range (41.8–58.8°C). Varying speckle patterns were acquired at known temperatures in both cases. The initial pattern was considered as reference and two statistical parameters were computed. Graphs were formed by implementation of two algorithms and analyzed to examine the speckle behaviour in terms of working range and sensitivity. References were also shifted during analysis for confirmation of the results regarding dynamic range.

### 6.1. MSV & Correlation in Single-turn Configuration

Fig. 5 shows that normalized MSV increases monotonically from zero as the temperature increases till a saturation point is reached. Interestingly, this behaviour is seen when any other point is taken as reference. Six such references were considered before the saturation temperature was reached. The graphs show that at any reference temperature, the sensor may be characterised with parameters such as sensitivity, dynamic working range and linear working range that are calculated from the graphs. Alternatively, the reference may be shifted before to extend the working range with some accumulated error [1].

Using the first curve, dynamic range was found to be approximately 13.1°C (35°C to 48.1°C), while linear range ($\Delta T$) was found to be 4.9°C (35°C to 39.9°C) with temperature sensitivity ($\Delta MSV/\Delta T$) of 0.0070°C$^{-1}$. Other curves using MSV for single-turn configuration provided dynamic ranges 10.6°C, 13.2°C, 12.4°C and 8.7°C respectively.

Similar observations are made using correlation except that it monotonically falls from unity as the temperature increases and the behaviour is also not as linear as with MSV. Fig. 6 provides a similar set of six curves with dynamic range 13.9°C (35°C to 48.9°C) and linear range of 6.6°C. In this linear range, the change in Correlation ($\Delta C$) is 0.030573 with sensitivity of 0.0046°C$^{-1}$. Other curves using correlation for single-turn configuration provided dynamic ranges 13.1°C, 13.6°C, 13.4°C, and 12.7°C respectively. It is evident that these ranges using correlation are more uniform than those obtained using MSV.

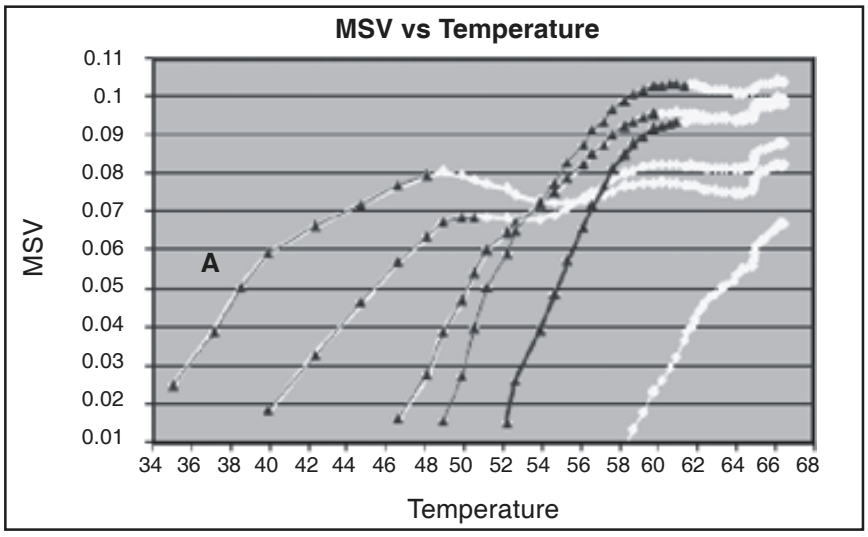


**Figure 5: MSV v/s Temperature (°C) in Single-turn Configuration**

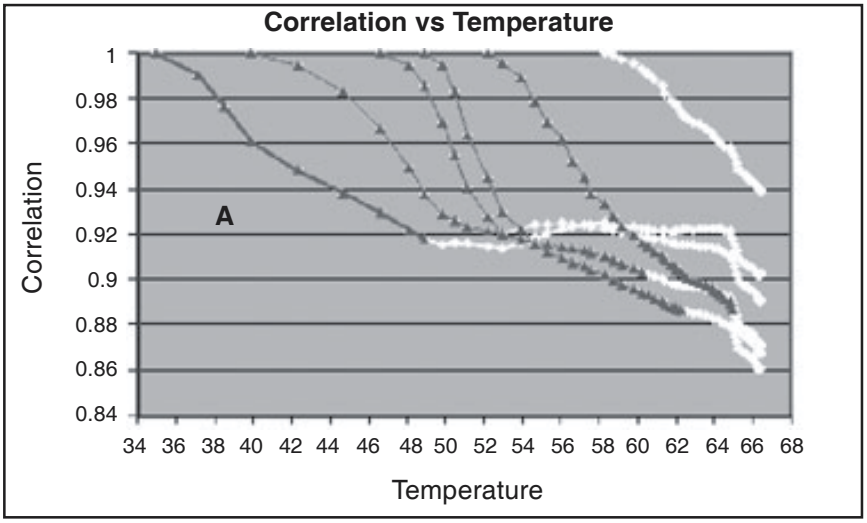


**Figure 6: Correlation v/s Temperature (°C) in Single-turn Configuration**

### 6.2. MSV & Correlation in Three-turn Configuration

Similar results were obtained using three-turn configuration for the experiment (41.8-58.8°C) and are shown in Fig 7 and 8. All the results from both the experiments are further summarised in Table I. Other curves using MSV for three-turn configuration provided dynamic ranges 6°C, 8.9°C, 7.7 °C, and 6.9°C respectively. While other curves using correlation also provided the same dynamic ranges of 6°C, 8.9°C, 7.7 °C, and 6.9°C respectively. It indicates that with the increase in sensitivity in three-turn configuration, the dynamic ranges are reduced and are similar for both MSV and correlation.

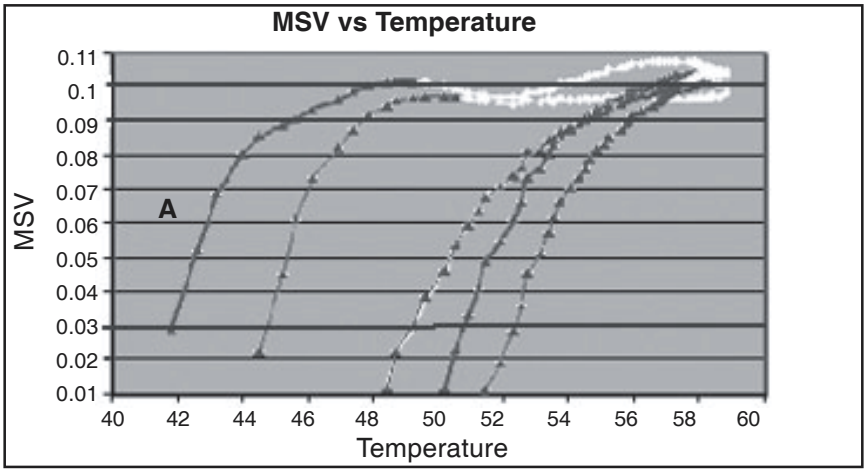


**Figure 7: MSV v/s Temperature (°C) in Three Turn Configuration**

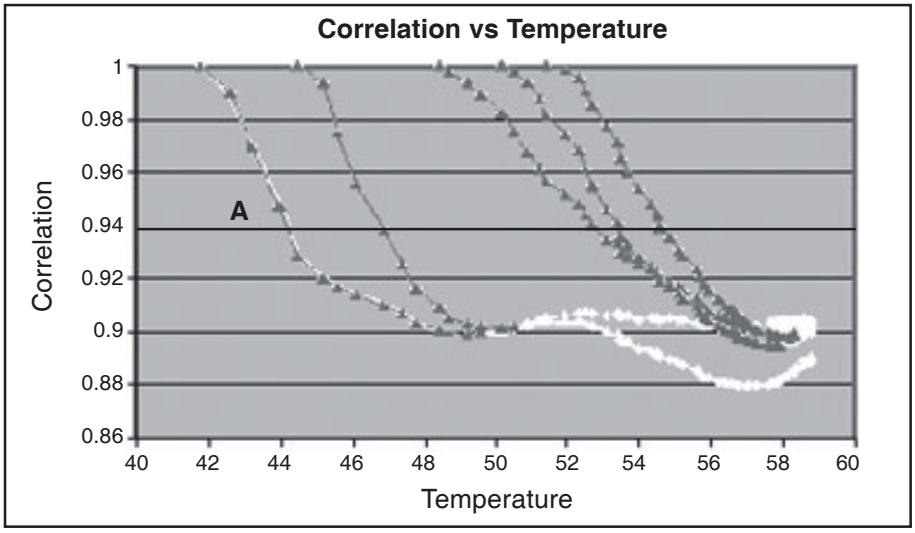


**Figure 8: Correlation v/s Temperature (°C) in Three-turn Configuration**

From the parameters calculated, it has been found that the three-turn configuration shows higher sensitivity and lesser dynamic range in comparison to single-turn configuration using either MSV or correlation. It can also be concluded that

**Table 1**
**MSV and Correlation v/s Temperature (°C)**

| **MSV** | | | |
|---|---|---|---|
| *Dynamic Range Curve A(°C)* | *Change in MSV (ΔMSV)* | *Linear working range (ΔT in °C)* | *Sensitivity ($°C^{-1}$)* |
| **Single-turn Configuration** | | | |
| 35.0 to 48.1, 13.1°C | 0.034552 | 35 – 39.9= 4.9 | 0.0070 |
| **Three-turn Configuration** | | | |
| 41.8 to 49.2, 7.4°C | 0.040169 | 43.2 – 41.8= 1.4°C | 0.0286 |
| **Correlation** | | | |
| *Dynamic Range (°C)* | *Change in Correlation (ΔC)* | *Linear working range (ΔT in °C)* | *Sensitivity ($°C^{-1}$)* |
| **Single-turn Configuration** | | | |
| 35.0 to 48.9, 13.9°C | 0.030573 | 48.9 – 42.3= 6.6 | 0.0046 |
| **Three-turn Configuration** | | | |
| 41.8 to 49.6, 7.8°C | 0.014782 | 47.8 – 44.5= 3.3 | 0.0044 |

correlation shows higher working range than MSV in both configurations, but is lower in sensitivity.

### 6.3. Response Time for Single-turn & Three-turn Configuration

One of most important practical parameter to characterize a sensor is response time. Response time of a sensor can be simply defined as how fast it responds to changes occurring in physical input. Two experiments were performed again for the two sensor configurations already chosen. Further, data was collected in two phases. In the first phase (A) when no heating was made, optimization of all system constraints for frame capture rate, was achieved. In the second phase (B), data collection was made at the same frame rate but with the optimum heating rate for both the configurations. The

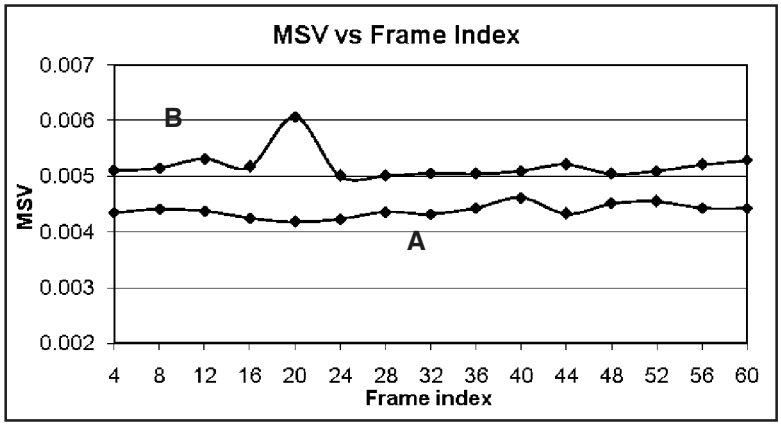


**Figure 9: MSV (with Every 4th Frame) vs. frame Index (Single-turn Config)**

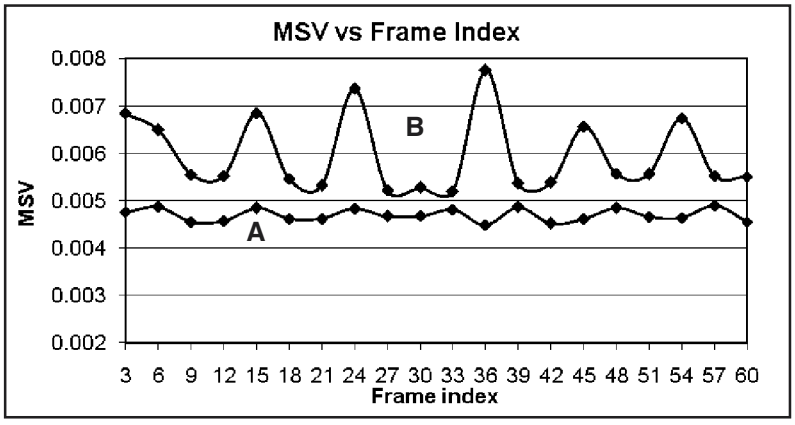


**Figure 10: MSV (with Every 3rd Frame) vs. Frame Index (Three-turn Config)**

optimised real-time acquisition was 30frames/sec and the optimised temperature rise was 0.2°C/sec. A total of 60 frames were acquired at the optimum rate of rise in

As is evident, a practical limit for response time was to be ascertained in the presence of noise occurring when no heating is carried out. Therefore, while plotting the graphs MSV or correlation values were computed by attempting to use the $n^{th}$ number of frame as reference. As we shall see such analytical results were obtained to provide a detectable difference between 'heating (B)' and 'no heating (A)'. The value of $n$ was iteratively made available for the four cases as seen from various graphs.

In Fig. 9-12, both curves (A&B) are shown using MSV and correlation values for the two sensing configurations. The $x$-axis shows the indices of the image frames used during statistical computation of MSV or correlation. In all cases, curve (A) shows

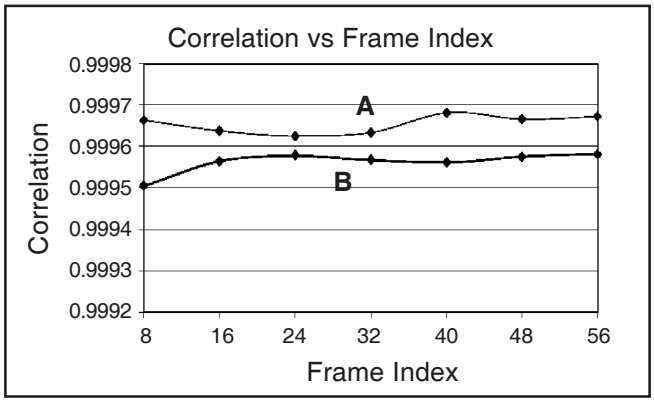


**Figure 11: Correlation (with Every 8th Frame) vs Frame Index (Single-turn Configuration)**

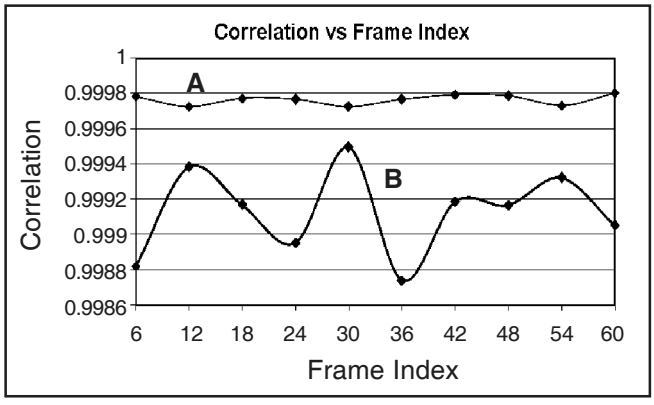


**Figure 12: Correlation (with Every 6th Frame) vs Frame Index (Three-turn Configuration)**

nominal variations in statistical parameter when no heating was carried out. All the points on the curves are indicating the MSV or correlation with reference to neighbourhood of $n^{th}$ *previous* frame, *i.e.* leaving $n$-1 frames in-between. The appropriate values of $n$ was found to generate a minimum detectable difference between signal (heating, B) and noise (no heating, A).

In Fig 9, curve B shows 15 points MSV plotted with reference to every $4^{th}$ ($n = 4$) until we got some clearly defined threshold. It shows that curve 'A' lies above 0.005 whereas curve B lies between 0.0041 to 0.0047. So a threshold is achieved in terms of MSV variations at 0.005; variations above 0.005 are due to temperature perturbations and the rest are due to noise. The same threshold (0.005) can be seen from Fig. 10 for three-turn configuration; though due to high sensitivity already observed, faster response time ($n = 3$) is observed. Similarly, using correlation for single-turn and three-turn configurations, a threshold of 0.9996 was obtained though for larger values of $n$, indicating slower response in both cases. From Fig. 11 and 12 these values are $8^{th}$ and $6^{th}$ frame for single- and three-turn configuration respectively.

**Table 2**
**Response Time (sec) and Sensitivity (°C)**

| | *Single-turn* | | *Three-turn* | |
|---|---|---|---|---|
| | *MSV* | *Correlation* | *MSV* | *Correlation* |
| Threshold | 0.005 | 0.9996 | 0.005 | 0.9996 |
| Response | 2/15sec | 4/15sec | 1/10sec | 1/5sec |
| Sensitivity | 0.0267°C | 0.0533°C | 0.02°C | 0.04°C |

Finally, since the temperature change was 0.2°C/sec after every 30 frames. For every $n^{th}$ frame, the response rate is 30/$n$Hz. For example, for three-turn sensor it is 1/10sec ($n = 3$) and 2/15sec ($n = 4$) for single-turn configuration using MSV. Similarly, using correlation, the response time is 1/5sec ($n = 6$) and 4/15sec ($n = 8$) for three-turn and single-turn respectively. Thus knowing the response time and the heating rate 0.2°C/sec, one can find the minimum detectable temperature (Sensitivity) using MSV or correlation in a single- or three-turn configuration. All these results are summarised in Table II. The system response time result shows that three-turn configuration is more sensitive and faster than single turn configuration. Similarly MSV is faster than correlation in two configurations.

## 7. CONCLUSION

In this paper, designing of speckle image based temperature sensing system and the characterization of its behaviour is performed. Two sensing configurations are designed

and analyzed for this purpose. The statistical parameters that are chosen for characterization of above said perturbations are Mean Speckle Intensity Variation (MSV) and Correlation. Different experiments are carried out on both configurations and their analysis and experimental results are obtained.

The results show that the sensor works for a maximum dynamic range using correlation in single-turn configuration. In the same configuration, MSV may also be used at higher sensitivity without much deterioration of the range. While using three-turn configuration, the saturation is reached early with lesser range due to higher sensitivity. The sensitivity and resolution has been computed in two experiments, namely change in MSV or correlation per unit temperature ($°C^{-1}$) and the minimum detectable temperature (°C) respectively. Considering the response time, the three-turn sensing configuration is faster than single-turn configuration. Further MSV allows easy detection of the minimum temperatures in comparison to correlation. The results show that the sensor can be used for precise measurements. It opens new possibilities in detecting, monitoring and analyzing thermal processes in various industrial installations and atmosphere, as well as in explosive units and oil refineries, where other electric sensors are unsafe. Further it is also concluded that fibre sensor works as field or area sensor for monitoring applications rather than conventional point sensors.

## REFERENCES

[1] Kun Pan, Chii-Maw Uang, Feng Cheng and Francis T.S.Yu, "Multi-Mode Fibre Sensing by Using Mean-Absolute Speckle Intensity Variations", *Applied Optics*, **33** (10), (April 1994), 2095–2098.

[2] W.B Spillman, Jr., B. R. Kline, L. B. Maurice, and P. L. Fuhr, "Statistical-Mode Sensor for Fibre Optic Vibration Sensing Uses", *Applied Optics*, **28**, (15), (August 1989), 3166–3175.

[3] Francis T. S. Yu, Kun Pan, Chii-Maw Uang, Paul B. Ruffin , "Fibre Specklegram Sensing By Means of An Adaptive joint Transform Correlator", *Optical Engineering*, **32** (11), (Nov 1993), 2884–2888.

[4] A Salvarajan and A. Asubdi, "Photonics, Fibre Optic Sensor and their Smart Structures" *Non-Destructive Evaluation*, J. 15(2).

[5] Eric UDD, "Fibre Optic Sensor: An Introduction for Scientists and Engineers" John Wiely and Sons, NewYark, (1991).

[6] R.S. Sirohi, "Selected Papers on Speckle Metrology" *SPIE Milestone Series* **35**, (1991).

[7] G. Burton, C. Joenathan, "Multi-Mode Optical Fibre Core Diameter Measurement Using Laser Speckles", *Optik*, **96** (1), (1994), 47–48.

[8] Juan A. Pomarico, Enrique E. Sicre, Dante Patrignani, Lorenzo De Pasquale, "Optical Fibre Strain Gauge based on Speckle Correlation", Elsevier, *Optics and Lasers Technology*, **31**, (1999), 219–224.

[9] Harish Kumar Sardana, Jagdish Kumar Chhabra, Somnath Bandyopadhyaya,; Pramod Kumar Goel, "Multi-fibre Optic 2D-array Device for Sensing and Localizing Environment Perturbation using Speckle Image Processing," *United States Patent* 6, 590,194, (July 8, 2003).

[10] Wai-On Wong, "Vibration Analysis by Laser Speckle Correlation", Elsevier, *Optics and Lasers in Engineering*, **28**, (1997), 277–286 .

[11] Yurl N. Kulchin, Oleg B.Vitrik, Oleg V. Kirichenko, Oleg T. Kamenev, Yurl S.Petrov, O.G Maksaev, "Method of Single Fibre Multi-mode Interferometer Speckle Signal Processing", *Optical Engineering*, **36** (5), (May 1997), 1494–1498.

**Bhasker Gupta**
ECE Dept
Chitkara Institute of Engineering and Technology
Punjab
INDIA
E-mail: *guptabhasker@gmail.com*

**H. N. Bhargaw & H. K. Sardana**
DU-2, Central Scientific Instruments Organisation
Chandigarh
INDIA